CHAPTER 1

INTRODUCTION TO SILICON CARBIDE (SIC) MICROELECTROMECHANICAL SYSTEMS (MEMS)

Rebecca Cheung

School of Engineering and Electronics
King's Buildings
University of Edinburgh
Edinburgh, EH9 3JL, Scotland, UK
E-mail: r.cheung@ed.ac.uk

This chapter serves as a brief introduction to the basic properties of silicon carbide (SiC) and the advantages of using SiC over other semiconductor materials for microelectromechanical systems (MEMS). Given the excellent and extensive review chapters that follow this one, I have confined this chapter to recent research performed at the University of Edinburgh in the area of SiC microelectromechanical systems (MEMS). Some of the processes involved in the fabrication of microelectromechanical systems in SiC are discussed, together with the problems to be overcome in order for SiC's potential as a MEMS material be exploited in applications for harsh environments.

1. Introduction

The total MEMS market worldwide already exceeds $10 billion, up from $100 million only five years ago.[1] Addressable markets include automotive, medical, telecommunications, industrial, transportation and environmental while consumer products include household appliances and toys. Currently, the most successful MEMS sensors are made in silicon. Examples include sensors that trigger the deployment of automotive airbags as well as ink jet nozzles. On the other hand, commercial MEMS in SiC is still in its infancy and occupies a niche

market. However, the future SiC MEMS market could become substantial, contributing a significant percentage of the total market for MEMS. Because of the unique material properties of SiC including wide bandgap, mechanical strength, high thermal conductivity, high melting point and inertness to exposure in corrosive environments, devices manufactured in SiC are more robust. Such SiC MEMS can operate at higher temperatures and in harsh environments compared to their silicon counterparts.[2,3] Potential new markets where SiC sensors could make a large impact include, for example:

(1) Radio frequency (rf) MEMS area for rf and millimetre wave applications in military, commercial wireless communication, navigation and sensor systems, where devices including micro-switches, tunable capacitors, micro-machined inductors, micro-machined antennas, micro-transmission lines and resonators made in SiC present potential improvements in operating frequency, power handling capability and reliability compared to devices made in silicon;

(2) Pressure sensors for use in the oil industry where currently, the procedure for oil drilling is modified in order to prevent sensors from physical damage due to the high vibrational environment;

(3) Accelerometers in aeroplane engines and motors in harsh environments for detecting acceleration, hence potentially providing better safety control;

(4) Optical MEMS (MOEMS) applied to general industrial applications for control of light, sensing and in manufacturing technologies.

RF MEMS is expected to be the third major player in the MEMS market, estimated to exceed $1 billion by 2007, while revenues for simple MEMS devices such as filters and inductors are predicted at a modest $200 million by 2007.[4] Long term reliability of components is believed to be the second most important issue after price. Therefore, SiC MEMS has extremely strong prospects as a key platform process. Similarly, optical MEMS for sensor systems is predicted to grow to $347 million in 2007 and $100 million for positioning and alignment systems.[5] The advantages of SiC for MOEMS is yet to be explored, but high stability is certainly one potentially exploitable parameter.

However, thus far, the difficulty in the growth and processing of the material has meant that progress in the use of SiC for MEMS applications has been slow. Nevertheless, in the past decade, tremendous efforts have been put into the growth and processing aspects of SiC and as a result, the application of SiC as a MEMS based material is beginning to appear attractive. The remaining chapters of this book combine to give an excellent review of the state-of-the-art technology and processes for the growth of SiC, contacts to SiC and etching of SiC, with the final chapter focussing on the applications of SiC MEMS.

2. SiC Material Properties

SiC exhibits a one-dimensional polymorphism called polytypism. All polytypes of SiC have an identical planar arrangement of Si and C atoms, which are distinguished by differences in the stacking sequence of the identical planes. Disorder in the stacking periodicity of similar planes results in a material that has numerous crystal structures (polytypes), all with the same atomic composition. The magnitude of the disorder is such that more than 250 SiC polytypes are identified to date.[6] Despite the large number of polytypes, only three crystalline structures exist: cubic, hexagonal and rhombohedral. The origin of the polytypism can be visualized as follows. In Figure 1, the solid circles represent spheres closely packed in a plane; call this "plane 1". To place another such set of spheres on top of plane 1 as closely as possible, one would place each sphere in the hole between any three neighbouring spheres in plane 1 (dotted circles, plane 2). But there is another way of accomplishing this: the dashed circles in plane 3. The order of stacking of the planes determines the types of close-packed structures and their symmetry properties. According to conventional nomenclature, a SiC polytype is represented by the number of Si-C double layers in the unit cell, the appending letter C, H, or R indicating a cubic, hexagonal or rhombohedral symmetry. For example, the 6H hexagonal lattice has six such layers in the primitive cell with the following succession of the above planes: 1,2,3,1,3,2,1,2,3,1,3,2; the 3C lattice is built up as 1,2,3,1,2,3; 2H-SiC corresponds to 1,2,1,2; and 4H-SiC corresponds to 1,2,1,3,1,2,1,3.

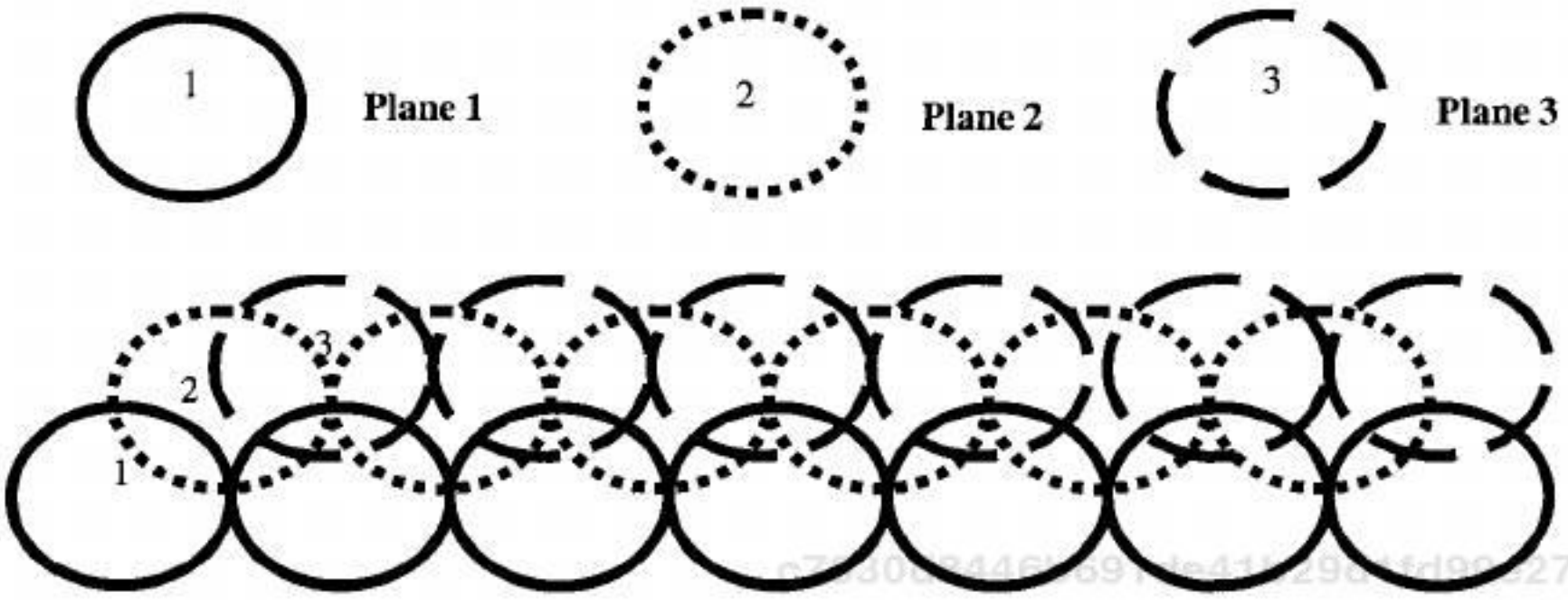

Figure 1. Schematic diagram of atomic arrangements in the different SiC polytypes (see text).

Although all SiC polytypes have the same atomic composition, the electrical properties differ. For instance, the bandgap for SiC ranges from 2.3eV for 3C-SiC to 3.4eV for 4H-SiC. Despite having the smallest bandgap, 3C-SiC has the highest electron mobility ($1000cm^2/Vs$) and saturation drift velocity ($10^7cm/s$), due in part to its cubic crystalline symmetry.

SiC has always been noted for its excellent mechanical properties, specifically, hardness and wear resistance. In terms of hardness, SiC has a Mohs hardness of 9, which compares favourably with values for other hard materials such as diamond (ten) and topaz (eight). In terms of wear resistance, SiC has a value of 9.15, as compared with 10.00 for diamond and 9.00 for Al_2O_2. SiC is not attacked by most acids and can only be etched by alkaline hydroxide bases (i.e. KOH) at molten temperatures (> 600°C). SiC does not melt, but sublimes at about 1800°C. The surface of SiC can be passivated by the formation of a thermal SiO_2 layer, even though the oxidation rate is very slow when compared with Si. The above properties are not generally polytype dependent. A comparison of the fundamental material properties of 3C-SiC, Si and 6H-SiC can be found on p.182 of this book and demonstrates the large potential of SiC MEMS as compared to silicon MEMS when applied in harsh environments.

3. Making a Microelectromechanical (MEM) Device

In order to make a microelectromechanical device, many aspects need to be considered including the growth of the required layers, design, processing, packaging and testing. SiC exists in different crystalline states, namely, single crystal, polycrystalline and amorphous. Different degrees of crystallinity can be grown on various substrates and as a result, a large combination of multi-layers containing SiC films can be possible and the processing for the final device of system depends on the layer design and the application. The chapters that follow provide an excellent overview of the constraints and possibilities in SiC film growth and processing for MEMS applications. In the following section, the two commonly employed processes including bulk and surface micromachining for MEMS applications are discussed.

3.1. Micromachining processes

3.1.1. Bulk micromachining

Conventional silicon bulk micromachining can be used for single-crystal, poly and amorphous SiC. For single-crystal SiC, the SiC must be grown directly on silicon. In this case, both front and back-side micromachining are possible as shown in Figure 2. Due to the high etch resistance of SiC, most commonly used anisotropic wet etchants can be used to remove the bulk silicon.

To improve reliability and control,[7-11] the group at Edinburgh has developed an all dry etch process for the bulk micromachining of 3C-SiC resonators on silicon.[12] A one-step inductively coupled plasma etch process using SF_6/O_2 gas mixture has been developed to fabricate straight resonators. The SiC resonators have been made first before the release of the cantilevers and bridges, performed by etching the silicon isotropically. The cantilevers and bridges have resonant frequencies between 120kHz and 5MHz depending on the device geometry; see Figures 3 and 4.

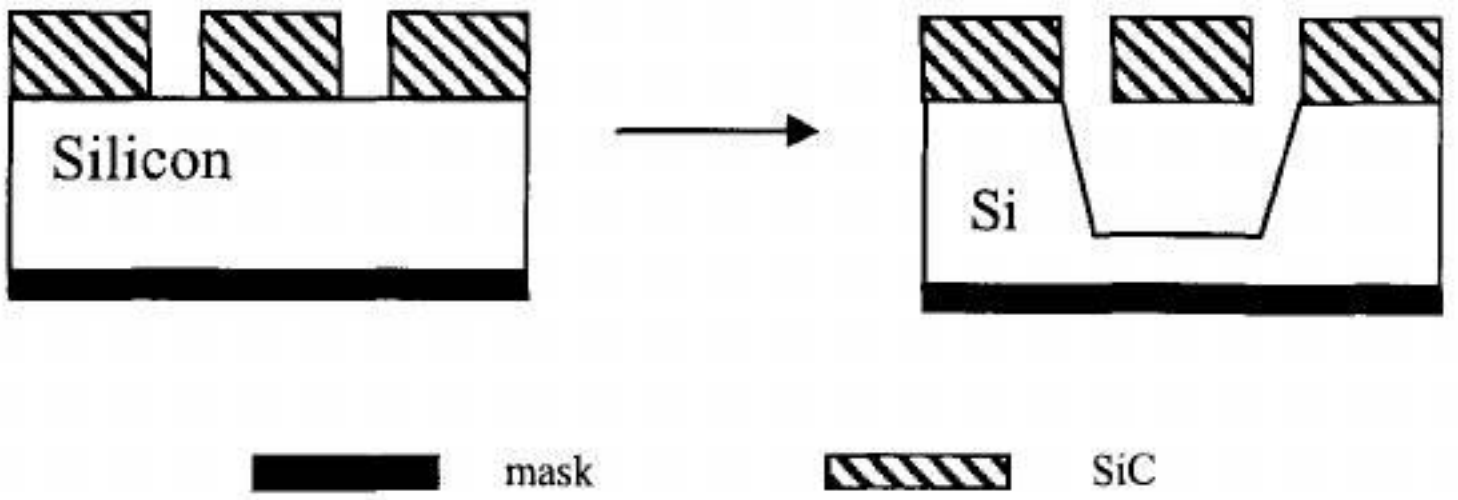

Figure 2(a). Bulk micromachining – release of SiC film via etching of silicon from the front of the wafer.

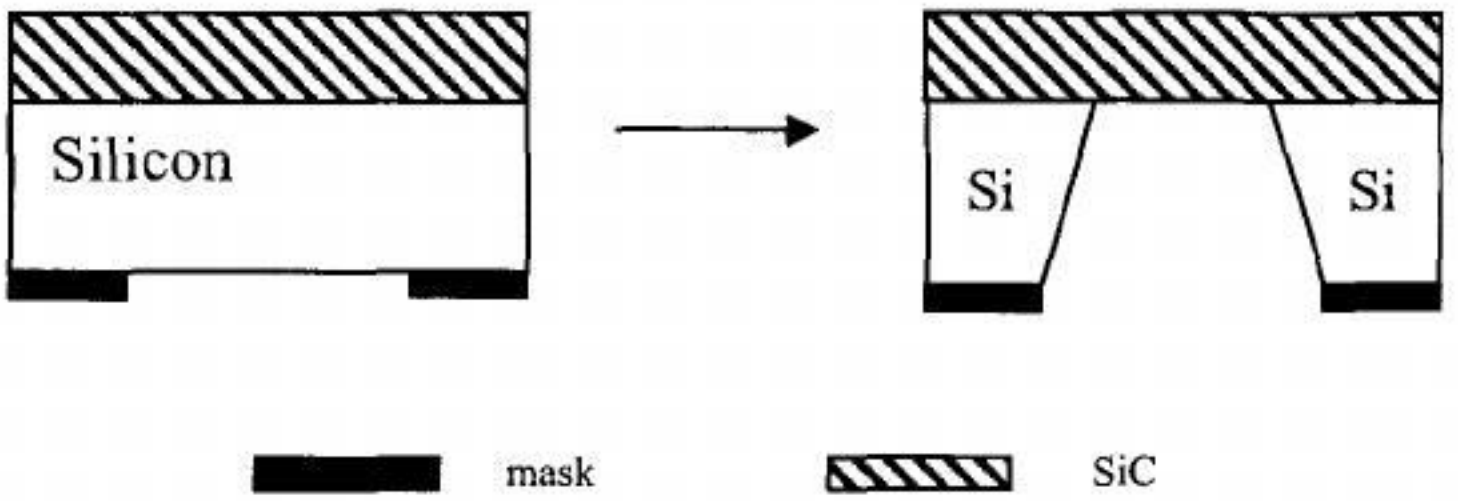

Figure 2(b). Bulk micromachining – release of SiC film via etching of silicon from the back of the wafer.

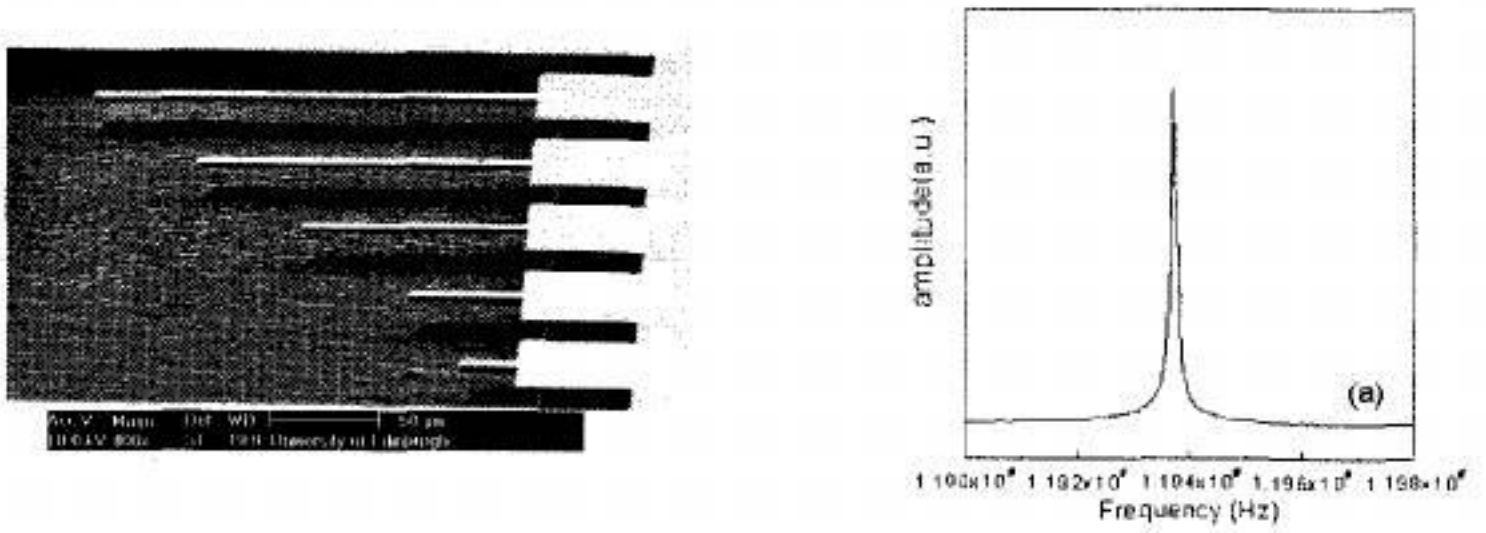

Figure 3. Array of SiC cantilever beams with lengths 25, 50, 100, 150, 200 μm, released from silicon using one-step dry etch process and the corresponding resonance response for the 200 μm cantilever beam.

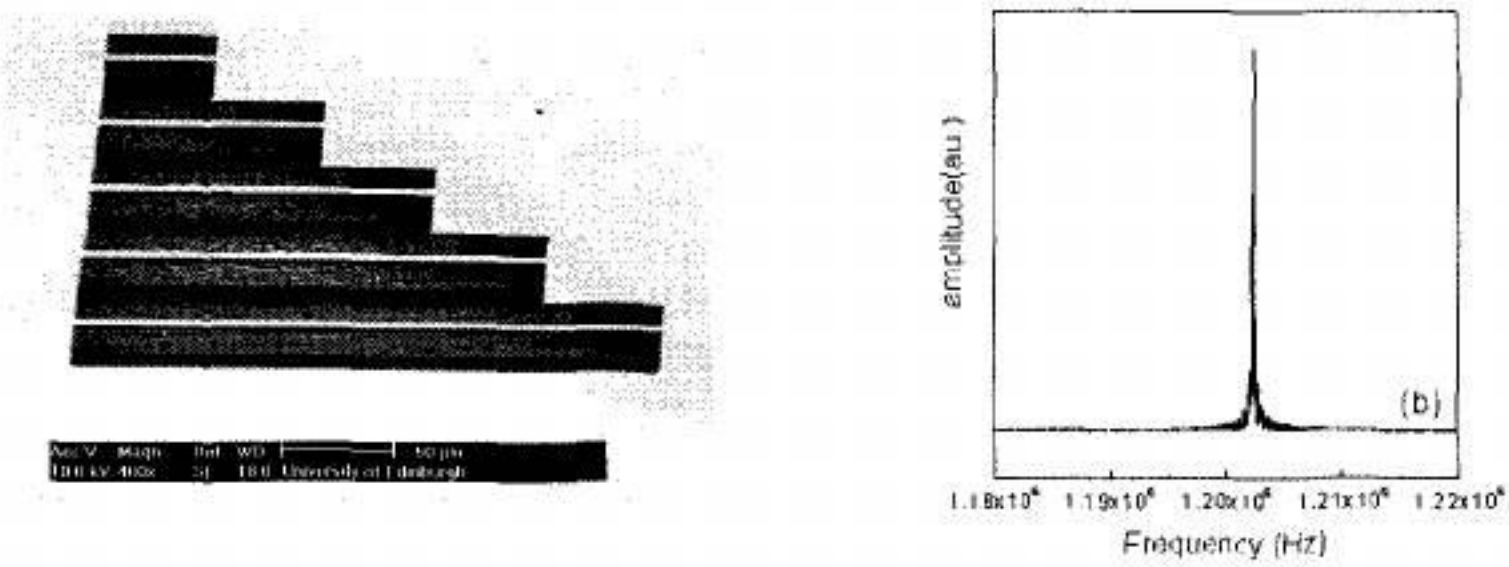

Figure 4. Array of SiC bridges with lengths 50, 100, 150, 200, 250 μm, released from silicon using one-step dry etch process and the corresponding resonance response for the 200 μm bridge.

3.1.2. Surface micromachining

The possibility to grow and process SiC films in multi-layer structures allows complex MEMS to be designed and processed and open doors to many applications. Similar wet or dry release processes employed for bulk micromachining can be used for surface micromachining also. For example, poly-SiC grown on a poly-Si layer or deposited on oxide layers, can be used as the mechanical layer while the poly-Si or oxide layer is used as the sacrificial layer, illustrated schematically in Figure 5. When poly-Si is used as the sacrificial layer, KOH, TMAH or our developed dry etch recipe can be used to release the SiC resonators, while the oxide is used to protect the underlying silicon during the sacrificial etch,[13] see Figure 6. An example of our fabricated resonator, 200 μm long, can be shown to be actuated electrostatically with a fundamental resonant frequency of 66.65kHz and an amplitude dependence on the applied V_{dc} and V_{ac} (Figure 7).[13] The processing of capacitively driven resonators and piezoresistive strain gauges on similar multi-layers[13-18] form the basis for more complex MEMS including accelerometers[19,20] and pressure sensors.[21-25] Further, for the first time, our 3C–SiC cantilever resonators have been shown to resonate upon electrothermal actuation.[26]

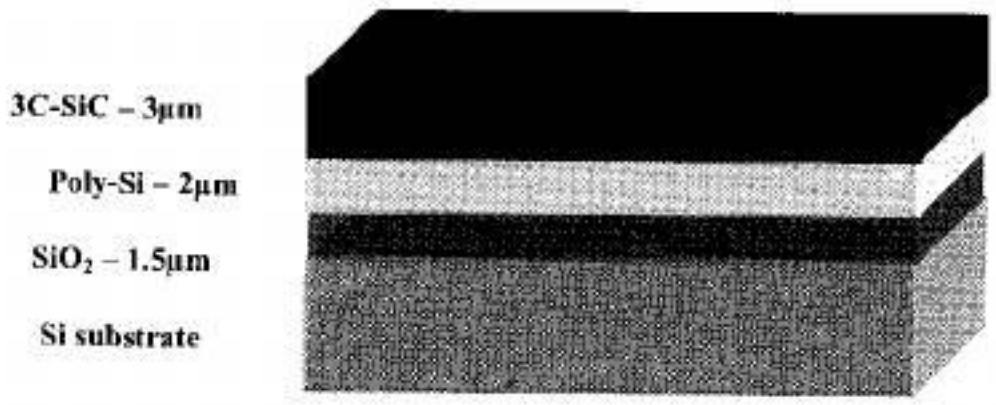

Figure 5. Multi-layer SiC/poly-Si/SiO_2/Si material structure.

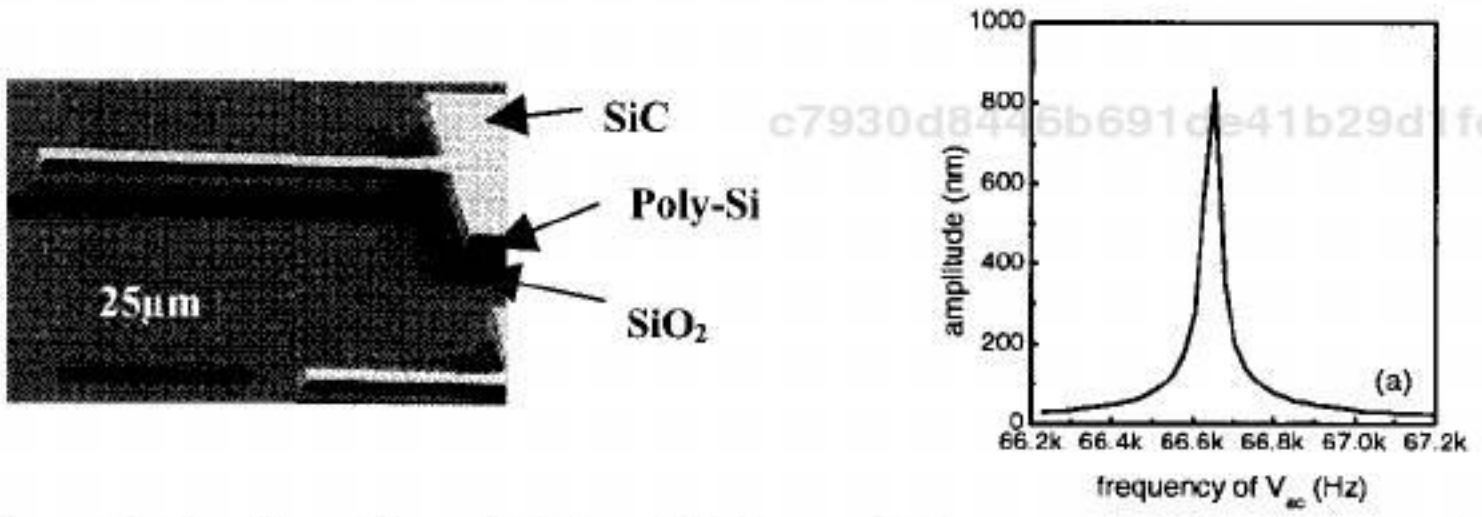

Figure 6. Cantilever beam fabricated in the multi-layer material structure and its corresponding fundamental resonant frequency.

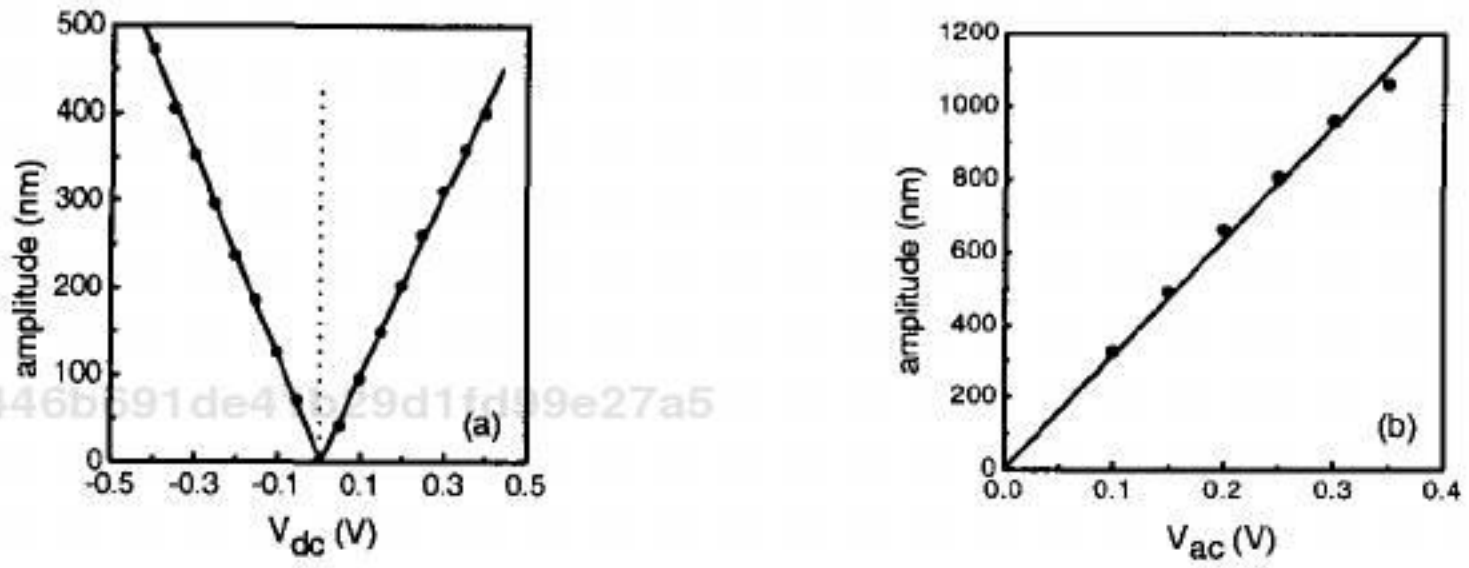

Figure 7. Amplitude Z for a 200 μm long cantilever as a function of: (a) V_{dc} (V_{ac}=0.3V), and (b) V_{ac} (V_{dc}=0.2V). The frequency of the applied a.c. signal was 66.65 kHz. The solid lines are linear fits to the data points.

4. Surface Modification

It has been reported recently that the surface microstructure of the MEM device can affect its response in particular the quality factor.[27] We have studied the surface modification at the microscopic scale after inductively coupled plasma etching of 4H-SiC in SF_6/O_2 using x-ray photoelectron spectroscopy.[28,29] Both C 1s and F 1s spectra from the

etched SiC under various etch conditions have been analyzed and studied. Our findings show the existence of both covalent and semi-ionic C-F bonds on the etched SiC surfaces, probably due to the existence of reactive F ions in the plasma. The intensities of the components of C-F groups in the C 1s spectra have been seen to decrease with the increase of O_2 in the gas mixtures, see Figure 8(a). The higher concentration of O_2 in the plasma would serve to remove C atoms thus leaving less C atoms available to react with F, causing the C-F groups in the C 1s spectra to become weaker with the increase of O_2 concentration in the SF_6/O_2 gas mixture.

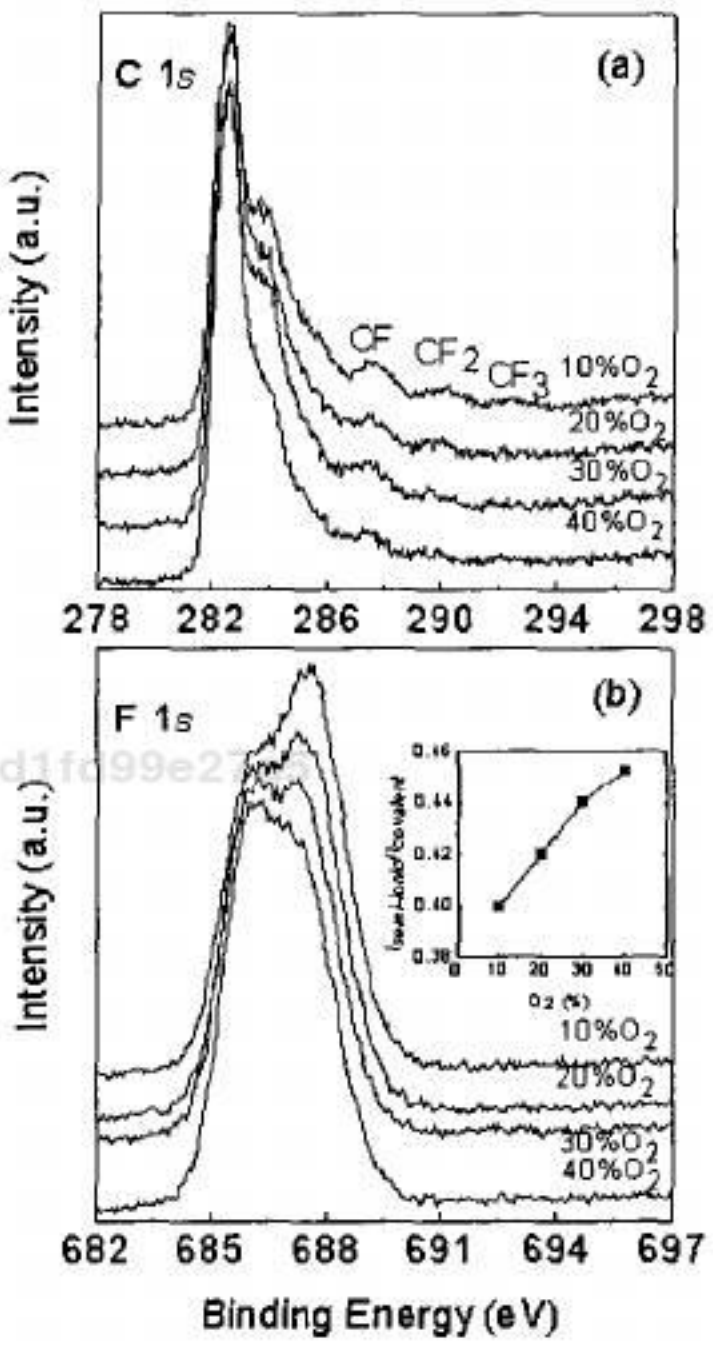

Figure 8(a). C 1s and (b) F 1s photoelectron spectra of SiC surface etched at different O_2 concentration in SF_6/O_2 gas mixture. The inset shows $I_{semi\text{-}ionic}/I_{covalent}$ ratio in the F 1s spectra as a function of O_2 concentration.

Figure 8(b) shows the F 1s spectra from the SiC etched at different O_2 concentrations in the SF_6/O_2 gas mixture. It can be seen that with the increase of O_2%, the dominant F 1s is changed gradually from covalent to semi-ionic C-F bonds. Shown in the inset is the increase in the relative $I_{semi\text{-}ionic}/I_{covalent}$ ratio with O_2% increase. In addition, it has been found that, in order to achieve higher etch rate of SiC, optimum O_2% in the SF_6/O_2 gas mixture and flow rate have to be applied during the dry etching of SiC. Furthermore, increasing chuck power and decreasing work pressure in the ICP system can also promote the etch processes. Figure 9 shows SiC etch rate and the F/Si ratio as a function of dc bias and chuck power, where larger etch rates are observed at higher dc bias and chuck powers. With the increase of chuck power, hence dc bias, more F incorporation is observed.

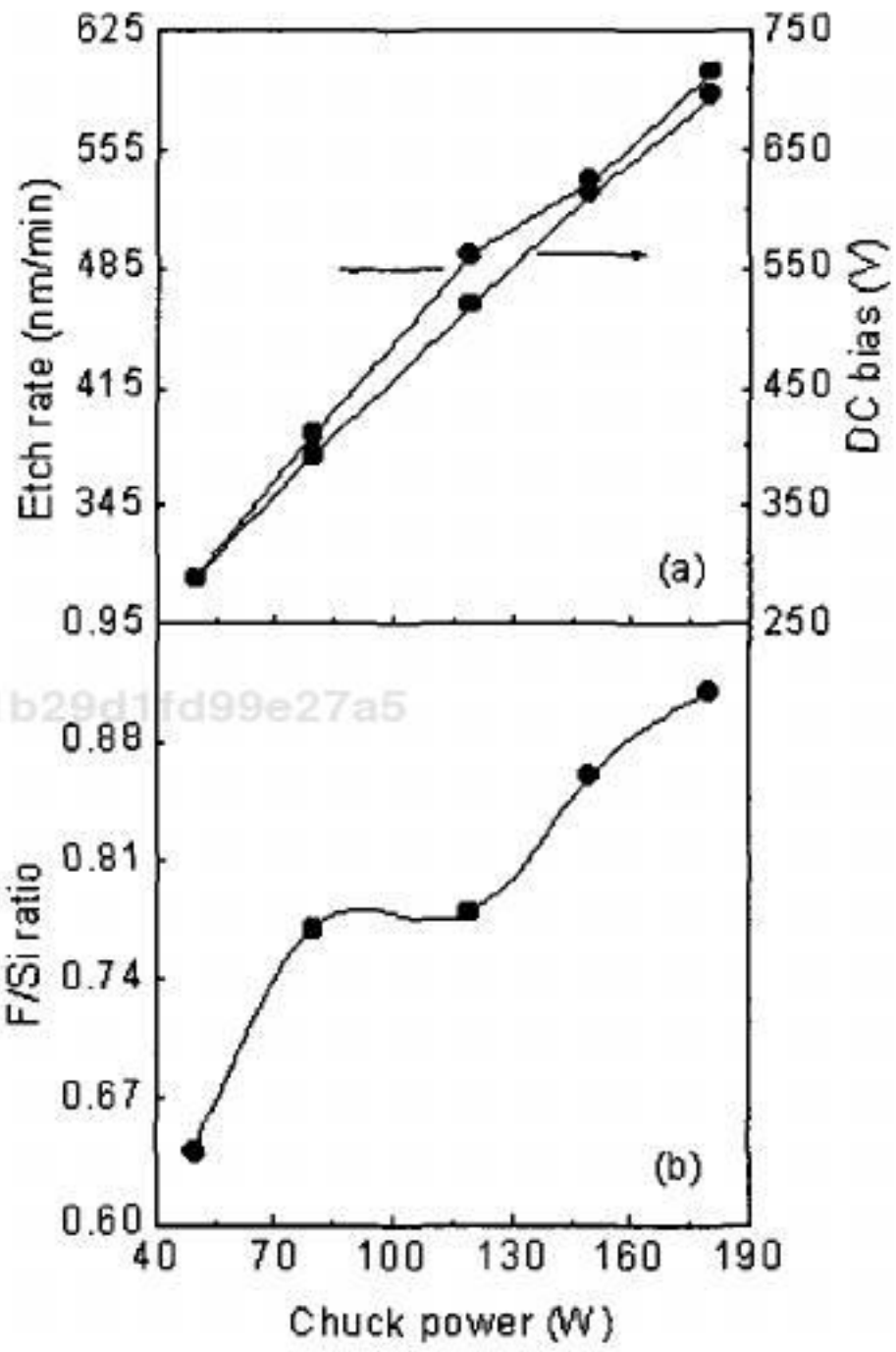

Figure 9(a). Etch rate and dc bias and (b) F/Si ratio vs applied chuck power. (SF_6 flow rate = 6-sccm, O_2 flow rate = 15sccm and pressure = 5mT).

From Figure 10(a), it can be seen that the intensities of the C-F bonds increase with the applied chuck power, particularly in the CF_2 bond. In addition, the CF_3 bond is observed only in the sample etched at 180W chuck power, while it is not obvious in the other two samples etched at lower chuck powers. These observations suggest that with the increase of the incorporated F concentration, the formation of C-F bonds is in the order of CF, CF_2, and CF_3, which is in agreement with the study of the growth of fluorinated carbon films.

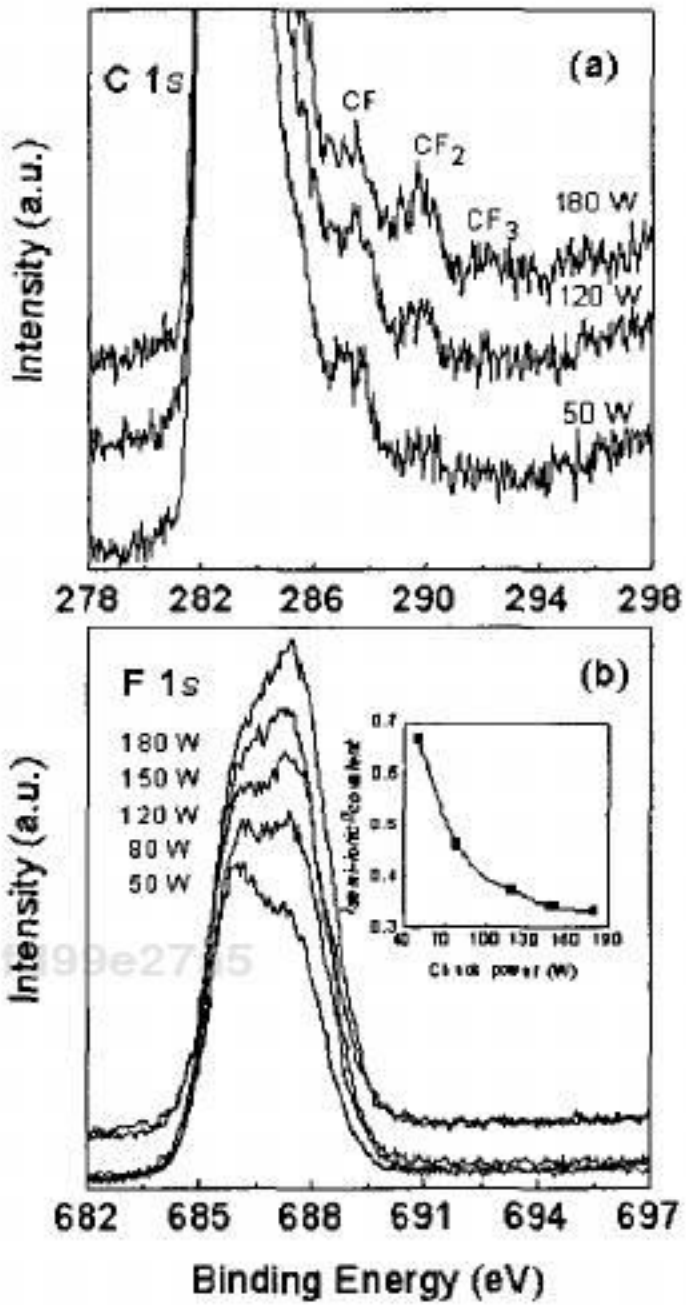

Figure 10(a). C 1s and (b) F 1s photoelectron spectra of SiC surface etched at different chuck powers. The inset shows $I_{semi\text{-}ionic}/I_{covalent}$ ratio in the F 1s spectra as a function of chuck power.

The F 1s spectra in Figure 10(b) show clearly the decrease of semi-ionic to covalent C-F bonds with an increase of the applied chuck power and etch rate, corresponding to the increase of the concentration of the incorporated F, as shown in Figure 9(b). Because of the difference in the electronic behaviour between semi-ionic and covalent C-F bonds,[30] our observation suggests that, SiC surfaces processed under lower etch rate conditions can become more conductive compared to those surfaces processed under higher etch rate conditions.

During the studies of F 1s spectra as a function of chuck power, pressure and SF_6 flow rates, it has been found that, in most cases, both the relative F concentration and the $I_{semi\text{-}ionic}/I_{covalent}$ ratio decreases as etch rate increases. Such microscopic surface modification on the subsurface could affect the MEM device performance such as the quality factor.[27] Moreover, the nature and quantities of the covalent and semi-ionic C-F bonds on the SiC etched surfaces, coupled with the complex etch mechanism of SiC,[31] can affect the performance of SiC electronic devices, as demonstrated in our recent study on the electrical behaviour of 4H-SiC Schottky diodes after inductively coupled plasma etching.[32-33] The effect of process–induced defects on the Schottky contacts is also discussed in Chapter 3.

5. Frequency Tuning of the SiC MEMS

More recently, our group demonstrated the resonant frequency tuning capability of SiC MEM resonators using focussed ion beam (FIB) deposited platinum (Pt),[34] see Figures 11 and 12. Platinum of surface area 13 x 5 μm^2 and thicknesses ranging from 0.3 to 3.1 μm has been deposited at room temperature on the cantilever and bridge resonators. The resonant frequency of the SiC cantilevers (Figure 11) and bridges (Figure 12) can be adjusted up to 12% by either adding platinum to or removing platinum from the resonators providing flexibility in tuning the resonant frequency when necessary.

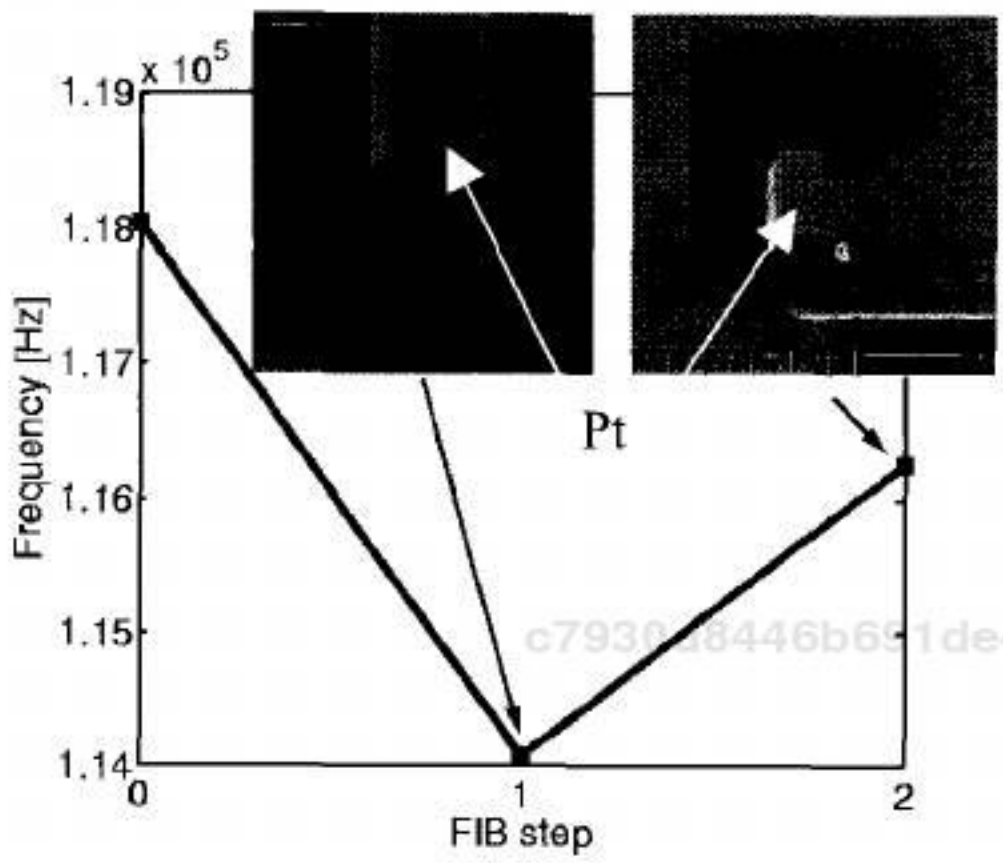

Figure 11. Change in frequency as a result of SiC cantilever (15 μm wide) tuning. FIB step 1: platinum deposition. FIB step 2: platinum milling.

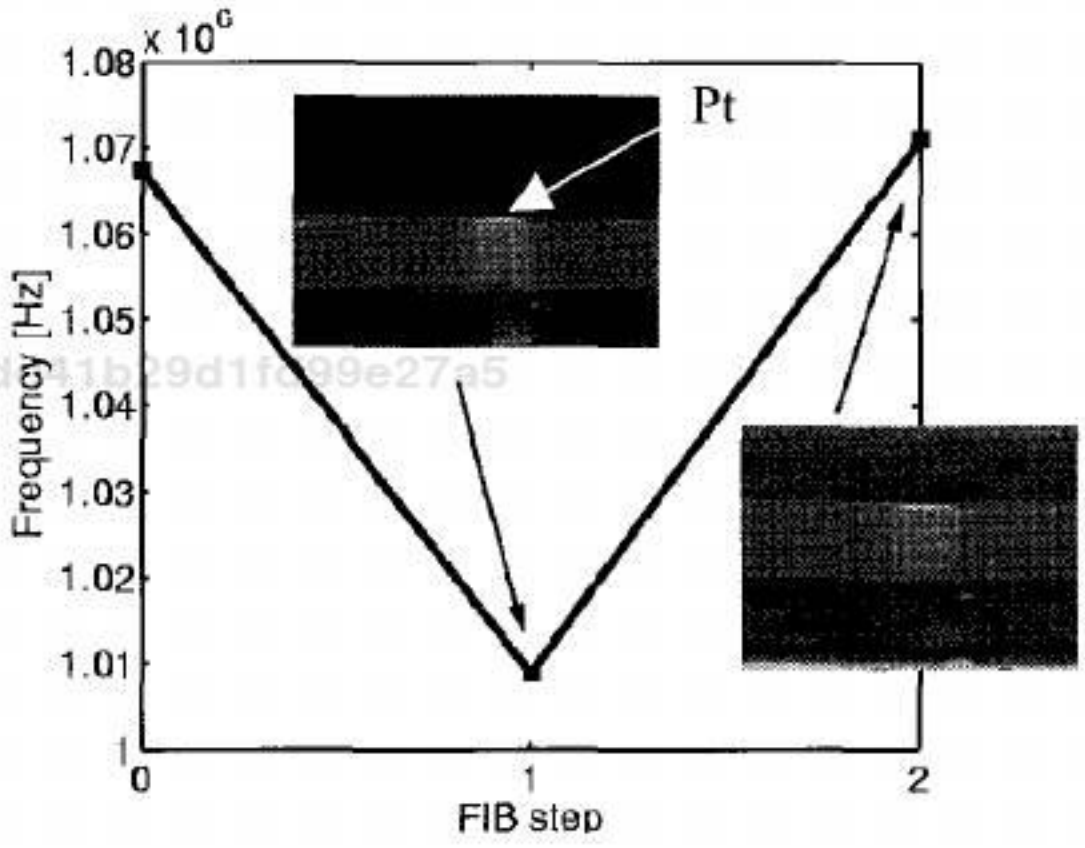

Figure 12. Change in frequency as a result of SiC bridge (15 μm wide) tuning. FIB step 1: platinum deposition. FIB step 2: platinum milling.

6. Mechanical Testing of the MEMS

Integrated MEMS require mechanical testing in addition to other forms of testing e.g. electrical, and can take the form of dimensional, dynamic and static tests. Optical techniques allow MEMS to be tested and modified precisely in a non-destructive manner. Figure 13 shows a schematic diagram of a workstation that contains a laser vibrometer for dynamic measurements, a surface profiler for static measurements and a Nd:Yag laser for laser ablation. Detailed operation specification of the workstation can be found in ref. 35.

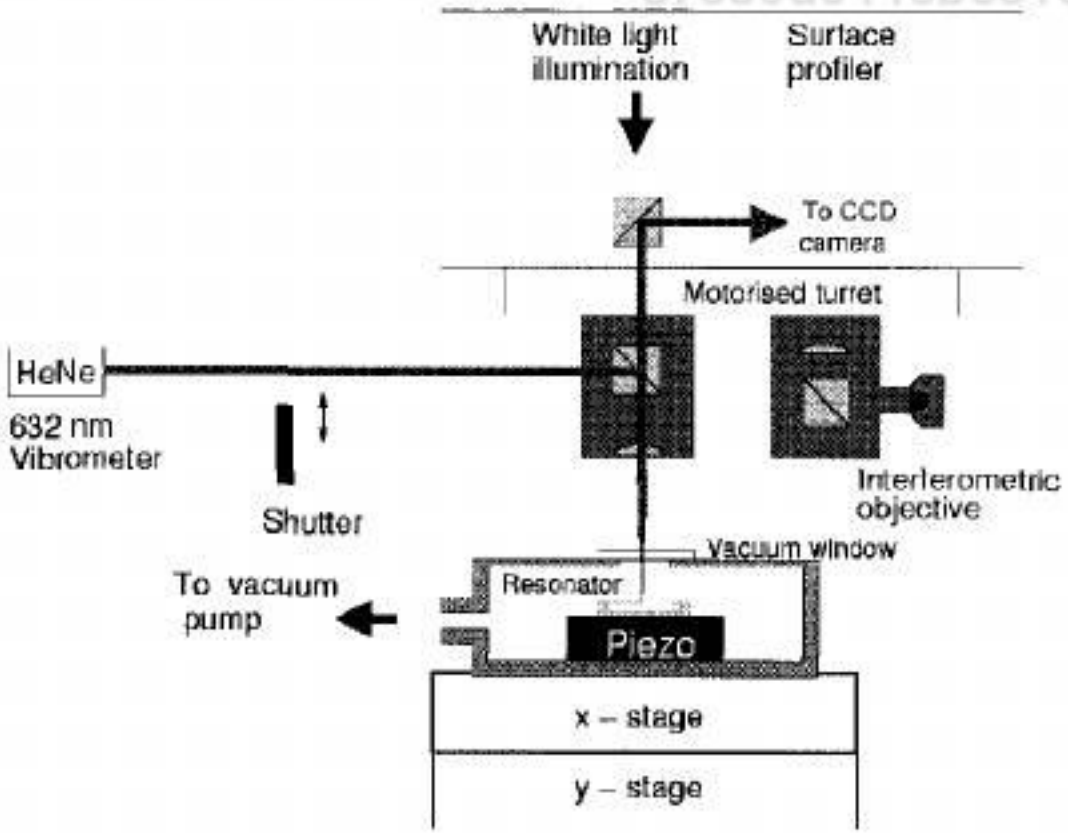

Figure 13. Optical workstation for resonator characterization.

7. Application Examples

Microelectromechanical systems based in silicon carbide, including accelerometer,[11,16] micro-motor,[36] pressure sensors,[21-25] gas sensors,[37,38] radiation detectors,[39] fuel atomizers,[40] have been demonstrated previously. For an excellent overview of the application areas of SiC, the reader is referred to chapter 5 of this book, which serves to illustrate in more detail the state-of-the-art SiC sensors, devices and systems that have been constructed so far.

Despite the large efforts devoted towards the research and development into SiC MEMS in the past decade, a lot remains to be done, especially in optimizing processes that are compatible with silicon, in order to reduce the cost of commercialization. A great impetus towards the future applications of SiC MEMS lies in its flexibility in integration with high temperature electronics. The possibility of MEMS and electronics that could operate at high temperatures and in harsh environments all in a single-chip module would no doubt enhance the commercialization prospects of MEMS in SiC.

8. Summary

This chapter has introduced the potential of using SiC as a MEMS material for harsh environments and has summarized the current research on SiC MEMS performed at Edinburgh. The future of SiC MEMS for harsh environments looks bright, especially when companies begin to commercialize SiC products[41] and as the understanding of the growth, etching and contact formation processes are advanced. The real potential of SiC MEMS applications will also be brought out when the integration of MEMS with electronics is proven.

REFERENCES

1. Hensler, R., Electronics.ca Publications, Research Report #GB270, BCC, (2002).
2. Mehregany, M., Zorman, C.A., Rajan, N. and Wu, C.H., *Proceedings of IEEE,* **86**, (1998), pp.1594-1610.
3. Sarro, P.M., *Sensors and Actuators,* **82**, (2000), pp.210-218.
4. Bouchaud, J. and Wicht, H., *Compound Semi & Microtechnology,* (2003), pp.26-29.

5. "Emerging Opportunities in Optical MEMS: 2003–2007", Communications Industry Researchers Inc., (2003).
6. Mirgorodsky, A.P., Smirnov, M.B., Abdelmounim, E., Merle, T. and Quintard, P.E., *Phys. Rev.*, **B52**, (1995), pp.3993-4000.
7. Fleishman, A.J., Zorman, C.A. and Mehregany, M., *J. Vac. Sci. Technol.*, **B16,** (1998), pp.536-539.
8. Pan, W.S. and Steckl, A.J., *J. Electrochem. Soc.*, **137,** (1990), pp.212-220.
9. Fleishman, A.J. *et al.*, *Proc. 9th Annual Int. Workshop on Microelectromechanical Systems*, San Diego, (1996), pp.473-478.
10. Fleishman, A.J., Wei, X., Zorman, C.A. and Mehregany, M., *Proc.7th Int. Conf. SiC III: Nitrides and Related Materials,* Sweden, (1997), pp.885-888.
11. Yasseen, A.A., Wu, C.H., Zorman, C.A. and Mehregany, M., *J. of Microelectromech. Systems*, **8**, (1999), pp.237-242.
12. Jiang, L., Cheung, R., Hassan, M., Harris, A.J., Burdess, J.S., Zorman, C.A. and Mehregany, M., *J. Vac. Sci. and Technol.*, **B21**, (2003), pp.2998-3001.
13. Jiang, L., Hassan, M., Cheung, R., Harris, A.J., Burdess, J.S., Zorman, C.A. and Mehregany, M., *Microelectronic Engineering*, **78-79**, (2005), pp.106-111.
14. Kuo, H.I., Zorman, C.A. and Mehregany, M., *Transducers '03: The 12th IEEE International, Conference on Solid-State Sensors, Actuators and Microsystems,* **2E86.P**, (2003), pp.742-745.
15. Shor, J.S., Goldstein, D. and Kurtz, A.D., *IEEE Transactions on Electron Devices,* **40**, (1993), pp.1093.
16. Wiser, R., Zorman, C.A. and Mehregany, M., *Transducers '03: The 12th IEEE International Conference on Solid-State Sensors, Actuators and Microsystems,* **3D3.5**, (2003), pp.1164-1167.
17. Roy, S., DeAnna, R.G., Zorman, C.A. and Mehregany, M., *IEEE Trans. on Electron Devices*, **49**, (2002), pp.2323-2332.
18. Yang, Y.T., Ekinci, K.L., Huang, X.M.H., Schiavone, L.M., Roukes, M.L., Zorman, C.A. and Mehregany, M., *Applied Physics Letters*, **78**, (2001), pp.162-164.
19. Okojie, R.S., Atwell, A.R., Kornegay, K.T., Roberson S.L., and Beliveau A., *Technical Digest of the 15th IEEE International Conference on MEMS*, Las Vegas, NV, (2002), pp.618-622.
20. Atwell, A.R., Okojie, R.S., Kornegay, K.T., Roberson S.L. and Beliveau A., *Nanotech 2002*, Puerto Rico, (2002).
21. Zappe S., Obermeier E., Möller H., Krötz G., Bonnotte E., Barriol Y., Decorps J.L., Rougeot C., Lefort O. and Menozzi G., *Conf. Transducers '99*, Sendai, Japan (1999), pp.346–349.
22. Zappe, S., Eickhoff, M. and Stoemenos, J., *Conf. Microelectronics, Microsystems and Nanotechnology,* Athens, Greece, (2000), pp.227-233.
23. Zappe, S., Franklin, J., Obermeier, E., Eickhoff, M., Moller, H., Krotz, G., Rougeot, C., Lefort, O. and Stoemenos, J., *Materials Science Forum*, **353-356** (2001), pp.753-756.
24. Eickhoff, M., Moller, H., Kroetz, G., Berg, J.V. and Ziermann, R., *Sensors and Actuators*, **A74**, (1999), pp.56-59.

25. Wu, C.-H., Stefanescu, S., Kuo, H.-I., Zorman, C.A. and Mehregany, M., *Conf. Transducers '01*, vol. 1, Munich, Germany (2001), pp.514-517.
26. Jiang, L., Cheung, R., Hedley, J., Hassan, M., Harris, A.J., Burdess, J.S., Zorman, C.A. and Mehregany, M., submitted to *J. Micromechanics and Microengineering*, (2005).
27. Huang, X.M.H., Zorman, C.A., Mehregany, M. and Roukes, M.L., *Transducers '03: The 12th IEEE International, Conference on Solid-State Sensors, Actuators and Microsystems*, **2E81.P**, (2003), pp.722-725.
28. Jiang, L., Cheung, R., Brown, R. and Mount, A., *Journal of Applied Physics*, **93**, (2003), pp.1376-1383.
29. Jiang, L., Plank, N.O.V. and Cheung R., *Microelectronic Engineering*, **67-68**, (2003), pp.369-375.
30. Nanse, G., Papirsr, E., Fioux, P., Moguet, F. and Tressaud, A., *Carbon*, **35**, (1997), pp.175-194.
31. Plank, N.O.V., Blauw, M.A., van der Drift, E. and Cheung, R., *Journal of Physics D; Applied Phys.*, **36**, (2003), pp.482-487.
32. Plank, N.O.V., Jiang, L., Gundlach A.M. and Cheung, R., *Journal of Electronic Materials*, **32**, (2003), pp.964-971.
33. Plank, N.O.V., Jiang, L., Gundlach, A.M. and Cheung, R., Proceedings of the 4th European Conference on Silicon Carbide and Related Materials, 2002, *Materials Science Forum*, **433-436**, (2003), pp.689-692.
34. Enderling, S., Jiang, L., Ross, A.W.S., Bond, S., Hedley, J., Harris, A.J., Burdess, J.S., Cheung, R., Zorman, C. A., Mehregany, M. and Walton, A. J., presented at *Nanotech 2004*, Boston, (2004).
35. Hedley, J., Harris, A., Burdess, J. and McNie, M., *Proceedings of the SPIE*, **4408** (2001), pp.402-408.
36. Yasseen, A.A., Wu, C.H., Zorman, C.A. and Mehregany, M., *IEEE Electron Device Letts*, **21**, (2000), pp.164-166.
37. Shields, V.B., Ryan, M.A., Williams, R.M., Spencer, M.G., Collins, D.M. and Zhang, D., *Inst. Phys. Conf. Ser.*, no 142, Ch. 7, (1996), pp.1067-1070.
38. Spetz, A.L., Tobias, P., Barabzahi, A., Martensson, O. and Lundstrom, I., *IEEE Trans. on Electron Devices*, **46**, (1999), pp.561-566.
39. Strokan, N.B., Ivanov, A.M., Savkina, N.S., Strelchuk, A.M., Lebedev, A.A., Syvajarvi, M. and Yakimova, R., *J. of Applied Physics*, **93**, (2003), pp.5714-5719
40. Rajan, N., Mehregany, M., Zorman, C.A., Stefanescu, S. and Kicher, T.P., *J. of Microelectromech. Systems*, **8**, (1999), pp.251-257.
41. www.FLXMicro.com